

A second order scheme for solving optimization-constrained differential equations with discontinuities

Alexandre Caboussat and Chantal Landry

Abstract A numerical method for the resolution of a system of ordinary differential equations coupled with a mixed constrained minimization problem is presented. This coupling induces discontinuities of some time-dependent variables when inequality constraints are activated or deactivated. The ordinary differential equations are discretized in time and combined with the first order optimality conditions of the optimization problem. We use a second order multistep method based on a predictor-corrector Adams scheme to detect the discontinuities by extrapolation of the trajectories. Optimization features, namely a sensitivity analysis, are exploited to compute the derivatives of the optimization variables and track the discontinuity points. The main difficulty consists in the impossibility of defining an explicit event function to characterize the activation or deactivation of a constraint. The order of convergence of our method is proved when inequality constraints are activated and numerical results for atmospheric organic particles are presented.

1 Introduction

Dynamic optimization problems arise when coupling an optimization problem with ordinary differential equations. They appear for instance in computational chemistry. We present here a mathematical model and a numerical method for the simulation of dynamic phase transition for a single atmospheric aerosol particle that exchanges mass with the surrounding gas [1]. The mass transfer is described by ordinary differential equations while a mixed constrained minimization problem

Alexandre Caboussat

Alexandre Caboussat, Department of Mathematics, University of Houston, 4800 Calhoun Rd, Houston, Texas 77204-3008, USA, e-mail: caboussat@math.uh.edu

Chantal Landry

Chantal Landry, Institute of Analysis and Scientific Computing, Ecole Polytechnique Fédérale de Lausanne, 1015 Lausanne, Switzerland e-mail: chantal.landry@epfl.ch

determines the thermodynamic equilibrium of the particle, *i.e.* the partitioning of organics between different liquid phases.

Let $(0, T)$ be the interval of integration with $T > 0$. Let us denote by $\mathbf{b}(t)$ the concentration-vector of the s chemical components present in the particle at time $t \in (0, T)$. The dynamic optimization problem consists in finding $\mathbf{b}(t), \mathbf{x}_\alpha(t), y_\alpha(t)$ satisfying

$$\begin{aligned} \frac{d}{dt}\mathbf{b}(t) &= \mathbf{f}(\mathbf{b}(t), \mathbf{x}_\alpha(t)), \quad a.e. \ t \in (0, T), \quad \mathbf{b}(0) = \mathbf{b}_0, \\ (y_\alpha(t), \mathbf{x}_\alpha(t)) &= \arg \min_{\tilde{y}_\alpha, \tilde{\mathbf{x}}_\alpha} \sum_{\alpha=1}^p \tilde{y}_\alpha g(\tilde{\mathbf{x}}_\alpha) \\ \text{s.t. } \mathbf{e}^T \tilde{\mathbf{x}}_\alpha &= 1, \tilde{\mathbf{x}}_\alpha > 0, \tilde{y}_\alpha \geq 0, \alpha = 1, \dots, p, \quad \sum_{\alpha=1}^p \tilde{y}_\alpha \tilde{\mathbf{x}}_\alpha = \mathbf{b}(t), \end{aligned} \quad (1)$$

where p is the number of possible liquid phases present in the aerosol, \tilde{y}_α is the total number of moles in phase α , $\tilde{\mathbf{x}}_\alpha$ is the mole-fraction concentration vector in phase α , \mathbf{e} is the vector $(1, \dots, 1)^T$, g is the Gibbs free energy and \mathbf{f} is the mass flux between the aerosol and the surrounding media.

In the following sections we consider a model problem with linear equality constraints. Let $\mathbf{f}: \mathbb{R} \times \mathbb{R}^s \times \mathbb{R}^m \rightarrow \mathbb{R}^s$ be Lipschitz continuous and bounded, $g \in C^\infty(\mathbb{R}^m)$ and $A \in \mathbb{R}^{s \times m}$, with $s < m$. The problem reads: Find $\mathbf{b}: (0, T) \rightarrow \mathbb{R}^s$ and $\mathbf{z}: (0, T) \rightarrow \mathbb{R}^m$ satisfying

$$\begin{aligned} \frac{d}{dt}\mathbf{b}(t) &= \mathbf{f}(t, \mathbf{b}(t), \mathbf{z}(t)), \quad a.e. \ t \in (0, T), \quad \mathbf{b}(0) = \mathbf{b}_0, \\ \mathbf{z}(t) &= \arg \min_{\tilde{\mathbf{z}}} g(\tilde{\mathbf{z}}) \quad \text{s.t. } A\tilde{\mathbf{z}} = \mathbf{b}(t), \quad \tilde{\mathbf{z}} \geq 0. \end{aligned} \quad (2)$$

The loss of regularity of the variable \mathbf{z} occurs when one of the inequality constraints $z_i(t) \geq 0$, $i = 1, \dots, m$ is activated or deactivated. In this paper we only discuss the activation of constraints. The main difference between problems arising in control systems theory [10] and the present problem resides in the fact that the underlying energy g is minimized for *a.e.* $t \in (0, T)$ along the trajectory, and not only at the final time T .

The numerical scheme to solve (2) is introduced in the next section in the case without activation or deactivation of constraints. Then the algorithm for the detection of the discontinuities is presented. A theoretical result is given in a particular case and numerical results for the system (1) finally show the accuracy and efficiency of our method.

2 Numerical algorithm without tracking of discontinuities

In order to solve the system (2), we opt for a splitting algorithm between differential and optimization operators (see [1] for another approach). Hence we fully exploit

the characteristics of the minimization problem to ensure the admissibility of the solution.

The differential equations are solved with the Crank-Nicolson scheme. Let $h > 0$ be a fixed time step, $t^n = nh$, $n = 0, \dots, N$, the discretization of $(0, T)$ with $t^N = T$, and \mathbf{b}^n and \mathbf{z}^n denote respectively the approximations of $\mathbf{b}(t^n)$ and $\mathbf{z}(t^n)$. The differential equations discretized in time consist in finding $\mathbf{b}^{n+1} \in \mathbb{R}^s$ and $\mathbf{z}^{n+1} \in \mathbb{R}^m$ at each time step that satisfy

$$\frac{1}{h}(\mathbf{b}^{n+1} - \mathbf{b}^n) = \frac{1}{2}\mathbf{f}(t^n, \mathbf{b}^n, \mathbf{z}^n) + \frac{1}{2}\mathbf{f}(t^{n+1}, \mathbf{b}^{n+1}, \mathbf{z}^{n+1}). \quad (3)$$

We solve this equation with a fixed-point method. At each time step, a sequence of fixed-point iterates $(\mathbf{b}^{n+1, \ell}, \mathbf{z}^{n+1, \ell})$ is computed as follows:

- (i) setting $\mathbf{b}^{n+1, 0} = \mathbf{b}^n$ and $\mathbf{z}^{n+1, 0} = \mathbf{z}^n$,
- (ii) for $\ell = 0, \dots, r$
 - (a) solve the equation for $\mathbf{b}^{n+1, \ell+1}$ with a Newton method

$$\frac{1}{h}(\mathbf{b}^{n+1, \ell+1} - \mathbf{b}^n) = \frac{1}{2}\mathbf{f}(t^n, \mathbf{b}^n, \mathbf{z}^n) + \frac{1}{2}\mathbf{f}(t^{n+1}, \mathbf{b}^{n+1, \ell+1}, \mathbf{z}^{n+1, \ell}),$$

- (b) solve the optimization problem in (2) with $\mathbf{b}^{n+1, \ell+1}$ to obtain $\mathbf{z}^{n+1, \ell+1}$,
 - (c) if $\|\mathbf{b}^{n+1, \ell+1} - \mathbf{b}^{n+1, \ell}\|_2 \leq \text{tol} \cdot \|\mathbf{b}^{n+1, \ell+1}\|_2$ then return,
- (iii) set $\mathbf{b}^{n+1} = \mathbf{b}^{n+1, \ell+1}$ and $\mathbf{z}^{n+1} = \mathbf{z}^{n+1, \ell+1}$,

where r is a given maximal number of iterations and tol is a given tolerance.

Hence, at each iteration of the fixed-point method we have to solve the optimization problem to determine $\mathbf{z}^{n+1, \ell+1}$. The resolution of the optimization problem is based on a primal-dual interior-point method detailed in [2]. The main principle consists in relaxing the inequality constraint $\tilde{\mathbf{z}} \geq 0$ by adding a slack variable $\tilde{\mathbf{w}}$ that is incorporated into a logarithmic barrier term in the objective function. Let $\nu > 0$ be a given parameter. The minimization problem written as in the system (2) becomes

$$\begin{aligned} \min g(\tilde{\mathbf{z}}) - \nu \sum_{i=1}^m \ln(\tilde{w}_i) \\ \text{s.t. } A\tilde{\mathbf{z}} = \mathbf{b}, \quad \tilde{z}_i - \tilde{w}_i = 0, \quad \tilde{w}_i > 0, \quad i = 1, \dots, m. \end{aligned} \quad (4)$$

The objective function and the constraints of (2) being continuous, the solution of (4) converges to the solution of the initial problem (2) as ν tends to zero [6].

We write the first order optimality conditions corresponding to (4) in the fixed-point algorithm. After elimination of the slack variables, we obtain

$$\begin{aligned} \nabla g(\mathbf{z}^{n+1, \ell+1}) + A^T \boldsymbol{\lambda}^{n+1, \ell+1} - \boldsymbol{\theta}^{n+1, \ell+1} &= \mathbf{0}, \\ A\mathbf{z}^{n+1, \ell+1} &= \mathbf{b}^{n+1, \ell+1}, \\ z_i^{n+1, \ell+1} \theta_i^{n+1, \ell+1} - \nu &= 0, \quad i = 1, \dots, m, \\ z_i^{n+1, \ell+1}, \theta_i^{n+1, \ell+1} &> 0, \quad i = 1, \dots, m, \end{aligned} \quad (5)$$

where $\lambda^{n+1,\ell+1}$ and $\theta^{n+1,\ell+1}$ are dual (Kuhn-Tucker) multipliers.

Starting with an interior-point parameter v^0 , the above nonlinear system is solved by applying one Newton iteration, then decreasing the parameter $v^k = \xi v^{k-1}$, $\xi \in (0, 1)$, and repeating the process until convergence is reached [2, 6].

The interior-point method does allow constraints to be deactivated, since the solution of the relaxed minimization problem converges to the one of the original problem when $v \rightarrow 0$ [6]. From the numerical viewpoint, at each step of the algorithm, if $j \in \{1, \dots, m\}$ such that $|z_j^{n+1,\ell+1}| < \varepsilon$ exists (where ε is a given bound), then the j^{th} constraint is activated in the interval $[t^n, t^{n+1}[$.

3 Tracking of discontinuities

When an inequality constraint is activated or deactivated, the variable \mathbf{z} loses its regularity. In order to preserve the order of our numerical method, the discontinuity point has to be detected with enough accuracy [5, 7, 8]. An arising difficulty here is the absence of a function expressing explicitly the time when a constraint is activated, the variable \mathbf{z} being the result of a minimization problem for given \mathbf{b} .

The principle of our tracking method is an extrapolation method inspired by [4]. Let us assume that the j^{th} constraint $z_j(t) > 0$ activates and that the activation occurs during the interval $[t^n, t^{n+1}[$. We are looking for a fractional time step τ such that $z_j(t^n + \tau) = 0$. A Taylor expansion gives

$$0 = z_j(t^n + \tau) = z_j(t^n) + \tau \frac{dz_j}{dt}(t^n) + \mathcal{O}(\tau^2).$$

Hence, the time when the discontinuity occurs is estimated by

$$\tau \approx -z_j(t^n) / \frac{dz_j}{dt}(t^n). \quad (6)$$

The value $z_j(t^n)$ is already approximated by z_j^n , but the derivative $\frac{dz_j}{dt}(t^n)$ remains to be estimated. Starting from the chain rule

$$\frac{dz_j}{dt}(t^n) = \sum_{i=1}^s \frac{\partial z_j}{\partial b_i}(\mathbf{b}(t^n)) \cdot \frac{db_i}{dt}(t^n), \quad (7)$$

the approximation of the derivatives $\frac{\partial z_j}{\partial b_i}(\mathbf{b}(t^n))$ is derived with a sensitivity analysis [6]. The differentiation of the first order optimality conditions (5) with $v = 0$, relative to db_i , $i = 1, \dots, s$, leads to the linear systems for the variations of the solutions \mathbf{z}, λ due to a variation of the data b_i .

$$\begin{pmatrix} \nabla^2 g(\mathbf{z}) & A^T \\ A & 0 \end{pmatrix} \begin{pmatrix} \frac{d\mathbf{z}}{db_i} \\ \frac{d\lambda}{db_i} \end{pmatrix} = \begin{pmatrix} \mathbf{0} \\ \mathbf{e}_i \end{pmatrix}, \quad (8)$$

where \mathbf{e}_i is the usual unit vector defined by $(e_i)_k = \delta_{ik}$ for $k = 1, \dots, s$. The derivatives $\frac{\partial z_j}{\partial b_i}(\mathbf{b}(t^n))$ are approximated by

$$\frac{\partial z_j}{\partial b_i}(\mathbf{b}(t^n)) \approx \frac{dz_j}{db_i}(\mathbf{b}^n), \quad \text{for } i = 1, \dots, m. \quad (9)$$

The derivatives db_i/dt in (7) are approximated with the 2-steps Adams-Bashforth method with non-constant time step:

$$\frac{d}{dt}\mathbf{b}(t^n) \approx \mathbf{f}(t^n, \mathbf{b}^n, \mathbf{z}^n) + \frac{\tau}{2h} (\mathbf{f}(t^n, \mathbf{b}^n, \mathbf{z}^n) - \mathbf{f}(t^{n-1}, \mathbf{b}^{n-1}, \mathbf{z}^{n-1})). \quad (10)$$

Combining (6), (9) and (10) we obtain the following equation of second order in τ

$$0 = z_j + \tau \sum_{i=1}^s \frac{dz_j}{db_i} f_i(t^n, \mathbf{b}^n, \mathbf{z}^n) + \frac{\tau^2}{2h} \sum_{i=1}^s \frac{dz_j}{db_i} (f_i(t^n, \mathbf{b}^n, \mathbf{z}^n) - f_i(t^{n-1}, \mathbf{b}^{n-1}, \mathbf{z}^{n-1})),$$

that admits a unique positive root τ for a time step h sufficiently small.

Once the fractional time step τ is computed, a predictor-corrector method based on two-steps Adams-Bashforth and Adams-Moulton schemes is used to approximate \mathbf{b} at $t^n + \tau$, namely:

$$\begin{aligned} \mathbf{b}_{pred}^{n+1} &= \mathbf{b}^n + \tau \left[\left(1 + \frac{\tau}{2h}\right) \mathbf{f}(t^n, \mathbf{b}^n, \mathbf{z}^n) - \frac{\tau}{2h} \mathbf{f}(t^{n-1}, \mathbf{b}^{n-1}, \mathbf{z}^{n-1}) \right] \quad (\text{predictor}), \\ \mathbf{b}^{n+1} &= \mathbf{b}^n + \frac{\tau}{2} \left[\mathbf{f}(t^n + \tau, \mathbf{b}_{pred}^{n+1}, \mathbf{z}_{pred}^{n+1}) + \mathbf{f}(t^n, \mathbf{b}^n, \mathbf{z}^n) \right] \quad (\text{corrector}), \end{aligned}$$

where \mathbf{z}_{pred}^{n+1} is obtained by solving the optimization problem as in (2) with \mathbf{b}_{pred}^{n+1} . This method has a low computation cost, since all the terms in the above equations are already known before the tracking of the discontinuity except \mathbf{z}_{pred}^{n+1} in the corrector's equation, that has to be computed in addition.

4 Theoretical results

Error estimates for the approximations of the location and time when a discontinuity occurs are obtained in a simplified case by using nonlinear techniques presented in [3, 9]. We assume that (i) $\mathbf{z}(0) > 0$ and the j^{th} inequality constraint is the first to be activated in the time interval $(0, T)$ and (ii) the optimization algorithm [2] gives an exact solution.

Let us denote by t^* the first time when the event $z_j(t) = 0$ occurs and consider the particular case when the event is geometrically defined by the intersection of the trajectory $\mathbf{b}(t)$ with a given hyperplane of \mathbb{R}^s . We describe this plane by the parametric equations $\mathbf{O}\mathbf{C} + \sum_{i=1}^{s-1} \beta_i \mathbf{d}_i$, where \mathbf{O} is the origin of our axes, \mathbf{C} is a point in the hyperplane, \mathbf{d}_i , $i = 1, \dots, s-1$, are direction vectors and β_i , $i = 1, \dots, s-1$, are the unknown variables.

Let us define the function $\mathbf{F} : \mathbb{R} \times \mathbb{R}^{s-1} \rightarrow \mathbb{R}^s$ by $\mathbf{F}(t, \beta_1, \dots, \beta_{s-1}) = \mathbf{b}(t) - \mathbf{OC} - \sum_{i=1}^{s-1} \beta_i \mathbf{d}_i$. This function vanishes at the intersection point denoted by $(t^*, \beta_1^*, \dots, \beta_{s-1}^*)$.

Let \mathbf{b}_h be the linear spline interpolation of \mathbf{b}^n , $n = 0, \dots, N$. We define the numerical approximation $\mathbf{F}_h : \mathbb{R} \times \mathbb{R}^{s-1} \rightarrow \mathbb{R}^s$ by $\mathbf{F}_h(t, \beta_1, \dots, \beta_{s-1}) = \mathbf{b}_h(t) - \mathbf{OC} - \sum_{i=1}^{s-1} \beta_i \mathbf{d}_i$. The function \mathbf{F}_h vanishes at the approximated intersection point denoted by $(t_h^*, \beta_{1,h}^*, \dots, \beta_{s-1,h}^*)$.

As in the previous section we assume that there exists $n = n(h) \leq N - 1$ such that $t^* \in [t^n, t^{n+1}[$ (note that, when h becomes smaller, the index $n = n(h)$ becomes larger). We can establish the theorem (*a priori* error estimates):

Theorem 1. *Assume that the functions \mathbf{F} and \mathbf{F}_h admit zeros in $(0, T)$, denoted by $(t^*, \beta_1^*, \dots, \beta_{s-1}^*)$ and $(t_h^*, \beta_{1,h}^*, \dots, \beta_{s-1,h}^*)$ resp. Furthermore assume that \mathbf{b} can be extended in a C^3 manner in the neighborhood of the discontinuity point, and $D\mathbf{F}(t^*, \beta_1^*, \dots, \beta_{s-1}^*)$ is regular. Then:*

(i) *there exists $h_1 > 0$ and a constant $C_1 > 0$ such that*

$$\|\mathbf{F}_h(t^*, \beta_1^*, \dots, \beta_{s-1}^*)\|_\infty \leq C_1 h^2, \quad \forall h < h_1; \quad (11)$$

(ii) *there exist $h_2 > 0$, $\delta > 0$ and a ball centered in $(t^*, \beta_1^*, \dots, \beta_{s-1}^*)$ with radius δ , denoted by $\mathcal{B}((t^*, \beta_1^*, \dots, \beta_{s-1}^*), \delta)$, such that for all $h < h_2$ there exists a unique $(t_h^*, \beta_{1,h}^*, \dots, \beta_{s-1,h}^*) \in \mathcal{B}((t^*, \beta_1^*, \dots, \beta_{s-1}^*), \delta)$ satisfying $\mathbf{F}_h(t_h^*, \beta_{1,h}^*, \dots, \beta_{s-1,h}^*) = \mathbf{0}$. Moreover there exists a constant C independent of $h < h_2$ such that the following a priori error estimates holds*

$$\|(t^*, \beta_1^*, \dots, \beta_{s-1}^*) - (t_h^*, \beta_{1,h}^*, \dots, \beta_{s-1,h}^*)\|_\infty \leq C \|\mathbf{F}_h(t^*, \beta_1^*, \dots, \beta_{s-1}^*)\|_\infty. \quad (12)$$

The proof follows [3, 9]. Relationships (11) and (12) allow to conclude:

$$\exists h_0 > 0, C_0 > 0 \text{ s.t. } |t^* - t_h^*| + \|\mathbf{b}(t^*) - \mathbf{b}_h(t_h^*)\|_2 \leq C_0 h^2, \quad \forall h < h_0.$$

5 Numerical results

Numerical results for the detection of discontinuities are presented for the phase equilibrium problem (1) described in the introduction.

If the aerosol is a mixture of three chemical components, the solution \mathbf{b} of (1) and its numerical approximation can be represented on a two-dimensional phase diagram [2]. The phase diagram for a system composed by hexacosanol, pinic acid and water is illustrated in Figure 1 (a) where the digits (1,2,3) represent the number of deactivated constraints in each area.

In the particular case when all $y_\alpha(t)$ are strictly positive, the exact solution \mathbf{b} and the exact time of activation t^* when the third inequality constraint is activated are known. Starting from an initial aerosol composition of 20% of hexacosanol, 20% of pinic acid and 60% of water, and with a time step equals to 0.01s, we apply the algorithm of resolution with the tracking of the discontinuity. The numerical approx-

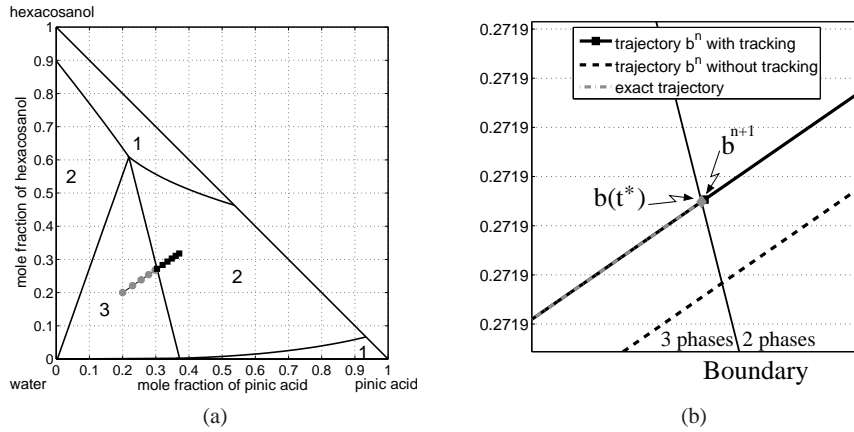


Fig. 1 (a) Numerical approximation of the trajectory of \mathbf{b} on the phase diagram of hexacosanol-pinic acid-water. (b) Zoomed-in view near the discontinuity point.

imation of \mathbf{b} is depicted in Figure 1 (a). The grey circles refer to the approximation \mathbf{b}^n when the three constraints are deactivated, whereas the black squares refer to \mathbf{b}^n with only two deactivated constraints. The number of activated constraints, and the discontinuity point located on the boundary between the areas with 3 and 2 activated constraints are accurately computed.

At each time step, the fixed-point algorithm stops in less than 3 iterations (for $tol = 10^{-5}$), while the interior-point method requires less than 25 iterations (for a tolerance of 10^{-13} on the increments in the infinity-norm), leading to a CPU time of 0.0028 s per time step with an Intel processor of 2.40 GHz.

Figure 1 (b) is a zoom of the trajectory of the numerical solution \mathbf{b}^n , $n = 0, \dots, N$, near the discontinuity point. The exact solution \mathbf{b} is represented, as well as the corresponding discontinuity point $\mathbf{b}(t^*)$, and the approximated trajectory of the numerical solutions with and without the tracking of the discontinuity. The discontinuity point obtained numerically is very close to the one obtained analytically and the trajectory with tracking is nearly superimposed with the exact trajectory, as opposed to the one without tracking.

Figure 2 (a) shows the evolution of the variables $y_\alpha(t)$, $\alpha = 1, \dots, 3$. The solid lines are the exact solutions y_1 , y_2 , and y_3 , whereas the markers \blacksquare , \blacklozenge and \bullet represent respectively the numerical values y_1^n , y_2^n and y_3^n for $n = 0, \dots, N$. The approximation of the time of the discontinuity is efficiently computed and markers are located at the point where the curves y_1 , y_2 and y_3 are not continuously differentiable.

Finally, Figure 2 (b) shows the convergence order for the error $|t^* - (t^n + \tau)|$ on the approximation of the time of the constraint activation t^* . This result numerically confirms that the method is convergent to the second order.

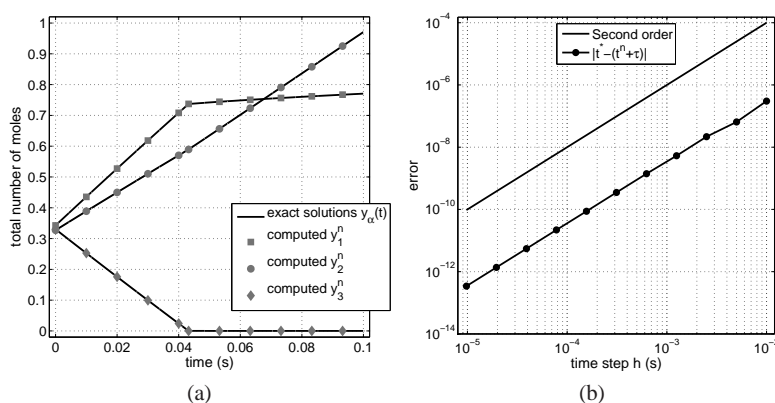


Fig. 2 (a) Plot of the exact solutions y_1, y_2 and y_3 . The markers \blacksquare , \blacklozenge and \bullet are respectively the computed values y_1^n, y_2^n and y_3^n for $n = 0, \dots, N$ (b) Log-log convergence plot of the error $|t^* - (t^n + \tau)|$.

References

1. Amundson, N., Caboussat, A., He, J., Landry, C., Seinfeld, J.H.: A dynamic optimization problem related to organic aerosols. *C. R. Math. Acad. Sci. Paris* **344**(8), 519–522 (2007)
2. Amundson, N., Caboussat, A., He, J.W., Seinfeld, J.H.: A primal-dual interior-point method for an optimization problem related to the modeling of atmospheric organic aerosols. *Journal of Optimization Theory and Applications* **130**(3), 375–407 (2006)
3. Caloz, G., Rappaz, J.: Numerical Analysis for Nonlinear and Bifurcation Problems, *Handbook of Numerical Analysis (P.G. Ciarlet, J.L. Lions eds)*, vol. 5, pp. 487–637. Elsevier, Amsterdam (1997)
4. Esposito, J.M., Kumar, V.: A state event detection algorithm for numerically simulating hybrid systems with model singularities. *ACM Transactions on Modeling and Computer Simulation (TOMACS)* **17**, 1–22 (2007)
5. Faugeras, B., Pousin, J., Fontvieille, F.: An efficient numerical scheme for precise time integration of a diffusion-dissolution/precipitation chemical system. *Math. Comp.* **75**(253), 209–222 (2005)
6. Fiacco, A.V., McCormick, G.P.: Nonlinear programming : sequential unconstrained minimization techniques. Wiley, New York (1968)
7. Gear, C.W., Østerby, O.: Solving ordinary differential equations with discontinuities. *ACM Trans. Math. Software* **10**(1), 23–44 (1984)
8. Hairer, E., Nørsett, S.P., Wanner, G.: Solving ordinary differential equations. I, *Springer Series in Computational Mathematics*, vol. 8, second edn. Springer-Verlag, Berlin (1993). Nonstiff problems
9. Rappaz, J.: Numerical approximation of PDEs and Clément’s interpolation. In: *Partial differential equations and functional analysis, Oper. Theory Adv. Appl.*, vol. 168, pp. 237–250. Birkhäuser, Basel (2006)
10. Veliov, V.: On the time-discretization of control systems. *SIAM J. Control Optim.* **35**(5), 1470–1486 (1997)